C.M. 1977/C:38

International Council for the Exploration of the Sea

Hydrography Committee

Airborne Infra-red Radiometry in the German Bight

by

G.A. Becker, K. Huber

Deutsches Hydrographisches Institut
Bernhard-Nocht-Str. 78
D2 Hamburg 4
Federal Republic of Germany

Radiométrie infrarouge dans la Baie Allemande à l'aide d'instruments aéroportés

Résumé.

Dans le cadre d'un "Remote Sensing Programme" on a examiné dans une région d'études dans la Baie Allemande dans quel mesure des capteurs IR de balayage sont capables de fournir des données sur la distribution de la température superficielle avec une précision satisfaisante. Les données obtenues par le balayage IR ont été traitées digitalement, ce qui a nécessité d'appliquer des procédés numériques étendus. Les résultats des premiers traitements révèlent que la correction de l'atténuation atmosphérique doit être améliorée. De plus, la différence entre la "skin temperature" et la température sub-superficielle doit être prise en considération si l'on fait une comparaison entre des températures de radiation infrarouge et des températures mesurées conventionnellement.

Abstract

Scanning I-R sensors were investigated in a testing area of the German Bight, within the framework of a Remote Sensing Programme, to see how far I-R sensors are suitable to obtain SST distributions with sufficient accuracy. The I-R scanner data were processed digitally, whereby extensive numerical procedures had to be employed. The results of the first processing show that the correction of the atmospherical attenuation must be improved. Furthermore, in comparisons between I-R radiation temperatures and conventionally measured temperature distributions, the temperature difference between the skin temperature and the subsurface measured temperature is to be taken into account.

Introduction

Within the framework of a German Remote Sensing Programme, scanning I-R sensors were investigated in a test area of the German Bight, to see how far they are suitable to obtain surface temperature distributions with sufficient accuracy ($\pm$ 0.2° C).

The I-R data were taken by a "DFVLR" * aircraft which - amongst other things - was equipped with a precision radiation thermometer (PRT 5, BARNES) and a multi-spectral scanner (M^2S, BENDIX). For correction and comparison of the I-R data obtained, extensive sea truth material was also obtained. The processing

---

Footnote: * "DFVLR" = Deutsche Forschungs- und Versuchsanstalt für Luft- und Raumfahrt e.V.

of the I-R data was carried out by the Authors, using a Digital Image Analysis System at the DFVLR in Oberpfaffenhofen. The primary results only are presented here, because of the extensive numerical problems occurring during the processing of the I-R data.

Observations

The inner German Bight between the light vessels "Elbe I" and "Deutsche Bucht", as well as between the light vessel "Weser" and the Island of Heligoland, were chosen as the testing area because, through the light vessels and Heligoland, salient points for the flight profiles were already in existence and comparison temperatures could be measured at these corner positions without the additional use of ships. Fig. 1 shows a chart of the German Bight with both flight profiles. The aircraft (DORNIER - Skyservant) flew over the profiles on 29th and 30th August, 1976, at three different altitudes (ca. 600 m; 1,200 m; 3,000 m). In the following, only the flight lane Heligoland - light vessel "Weser" at a flight level of 3,000 m on 29th August, 1976, is under consideration.

A weak wind (4 to 5 m/s), from an easterly direction, was blowing at the time of the flight. It was sunny, but hazy with - from time to time - slight overcast by clouds or high-lying, fog-type haze. R.V. "Gauß" was positioned at the point of intersection of the two profiles. The radiosondes started there, show for 29.8.1976 a high water-vapour content (Fig. 2), which to a

flight altitude of 3,000 m add up to 2.05 g cm^{-2} **, and thereby, in the H_2O window region from 8 to 14 μ cause a strong atmospheric attenuation in the I-R data. With a formula of Davis and Viezee (1967) which is valid for wave numbers from 8 to 12 cm^{-1}, the atmospheric transmission for water-vapour content was calculated as 0.762.

CTD measurements for the registration of the advective processes were carried out on board R.V. "Gauß" during the fly-overs. Furthermore, a Surface Rider Thermistor Chain was successfully employed, which registered - between 0.10 m and 3.30 m - with 22 thermistors the near-surface water temperature profile at timed intervals of 1 minute. Fig. 3 shows a water temperature profile during the fly-over. Rough estimates reveal that the longwave back radiation and the latent heat flux exceed the downwards-directed sensible heat flux. The heat balance, taking into account the heating of the surface layers by shortwave radiation, gives a temperature difference of $T_o - T_{25} \sim -0.2^o$ C. The water temperature profile shows a temperature inversion of about 1 m depth and confirms, thereby, the upwards-directed heat flux.

After the conclusion of the I-R aircraft plots, the distribution of the hydrographic parameters in the test strips was observed on board R.V. "Gauß" by running the scanned strips using a thermosalinograph and bucket.

Footnote: ** The meteorological data was obtained and evaluated by the Seewetteramt Hamburg.

Fig. 4 shows the quasi-synoptic subsurface temperature distribution in the test area gained thereby.

This distribution, taken in about 16 hours, is deformed by the strong tidal current, which is up to 1.5 sm/h in the German Bight. Thereby, an interpretation of the complicated horizontal temperature structure is made more difficult.

Owing to the run-off of the Elbe and Weser as well as to the East wind situation, warmer, low-saline North Friesian coastal water shifted towards the West. Simultaneously, colder and somewhat more saline water appeared at the mouth of the Weser, which probably originated from mixing with the colder bottom water. The arrangement of the isotherms and the isohalines (not shown here) suggests an anticyclonic eddy between the River Elbe, River Weser, and the Island of Heligoland.

Numerical methods

As Fig. 4 shows, only minor horizontal water temperature differences appeared in the test area, which reached a maximum of about 2° C. In order to resolve the weak gradients, the aircraft operator increased the scanner amplification, thereby spreading out the resolution. The result is a strong background noise, which superimposes upon the temperature signals; that is, the relationship of the signal to the noise is almost 1. For the digital treatment of the images, especially with regard to the formation of lines of equal temperature, it was necessary to smooth the images. For that reason, numerical filters were

developed, which were to separate the noise from the signal (Huber, 1978). The capacity of the computer equipment (DIBIAS, Oberpfaffenhofen) which was available for those computations, however, did not permit the use of two-dimensional filters. For that reason, at times, the rows and the lines were filtered separately.

For the determination of suitable filters, at first, lines and rows were Fourier analysed. Figs. 5a and 5b show the characteristic spectral properties of lines and rows. The figures present means from a large number of spectra. The spectrum of the radiation intensity taken from the scanner as a function of a relative wavelength is shown, the unit of which is the Pixel * distance. In the line direction the Pixel distance resp. the Pixel dimensions are not constant but angle-dependent. A plateau (white noise) is characteristic for all rows with lower wavelengths up to a wavelength of about 40 times the Pixel distance. Subsequently, in the direction of the larger wavelengths, there is a distinct broad peak (wavelength 40 times to 100 times that of the Pixel distance). This peak manifests itself in the images as an almost periodic strip structure in the row direction, and could possibly be interpreted as an instrument failure. The behaviour of the surface water temperature is described in the spectrum in the part with almost constant descent (in individual spectra, superimposed with peaks). One describes the spectrum in this region by the function:-

$$I_{(k)} \sim k^{-\alpha} \qquad (k = \text{wave number})$$

therefore, this gives for α:-

$$\alpha \sim 0.9.$$

---

* Pixel = picture (image) element.

Different filters were used in the rows: such with which one filtered off the transition band to white noise (peak at wavelengths of 40 to 100 Pixel distance) together with the white noise; or such which one considered in this region as relevant for the description of the temperature behaviour, and for that reason did not filter it off. Fig. 6b shows the spectrum of a row filter of the first type.

The spectra of the lines (Fig. 5a) distinguish themselves from those of the rows especially in that they have no distinct white noise plateau. Here, the noise concentrates in a distinct peak at wavelengths of about 5 Pixel distances. In general, the spectrum can be divided into two ranges, with different strong intensity descent. In many spectra in the transition band, there is a peak, the origin of which has not yet been clarified.

For the range of larger wavelengths in the rows, this results in

$$\alpha \sim 0.9.$$

For the range with smaller wavelengths, the result is

$$\alpha \sim 2.$$

The filter of the lines was so determined, in that wavelengths smaller than 6 Pixel distances were filtered out. The spectrum of that filter is shown in Fig. 6b.

For the correction of the atmospheric attenuation, the formula of Davis and Viezee was used for all Nadir angles of

the transmission. The corrections resulting therefrom, because of the DIBIAS internal data organization, were added row-wise. Finally, a geometrical correction - the Panorama Distortion Correction - was carried out.

Fig. 7 shows, in a flow diagram, the type and sequence of the numerical procedures used. After that processing, the digital image was given out over a line printer and as a pseudo colour image.

Results

In Fig. 8 the conventional and the radiometrical determined temperature distributions are compared. On principle, no conformity can be expected because of the different intervals of time at which they were taken. However, in both figures, the course of the isotherms and the order of magnitude of the gradients are comparable. The I-R image in absolute value lies about 1° C lower in the mean than the measured subsurface temperature distribution.

In the main, three reasons can be advanced for that:-

1) For the measured temperature difference between the air temperature and water temperature, the skin temperature lies about 0.2° C below that of the subsurface temperature (Hasse, 1963).

2) The atmospheric correction is too low, because of insufficient consideration of the wings of the H_2O window.

3) It was not taken into account that the water surface does not radiate as a black body. No non-blackness correction was used ($\sim 0.2^{\circ}$ C).

Furthermore, attention must be drawn to the fact that the digital filters slightly change the means of the images and, thereby, falsify the temperatures.

It is now being attempted to remove these errors in order to compare the radiometrical water temperatures direct with the conventionally observed water temperatures.

It will be attempted to gain better attenuation values using an atmospheric model of Selby and McClatchey (1972).

Furthermore, a non-blackness correction (Stevenson and Miller, 1974) will be used.

The temperature difference between the skin temperature and the subsurface temperature will be determined using a formular given by Hasse (1971)

$$T_o - T_w = C_1 \frac{H}{U} + C_2 \frac{Q}{U} \quad .$$

C_1; C_2 = empirical coefficients

H = heat flow

Q = solar radiation

U = wind speed

whereby, the heat flow at the interface will be estimated by a bulk formula given by Haney (1971).

Bulk formulas of Nagel (1971) are available for the calculation of the solar radiation.

The improvements of the evaluation procedures are not yet completed, owing to the considerable numerical procedures applied. However, we suppose that accuracy required ($\pm 0.2^{o}$ C) for the skin temperature can be attained.

Conclusions

Microstructures in the surface temperatures in areas with large temporal and/or local variability can be qualitatively recorded very well by means of I-R scanner images.

Structures become visible which cannot be realized by measurements from one or even several ships.

In estuaries, especially, or in coastal vicinities, mixing and transportation processes can be recorded by remote-sensing procedures.

In order to obtain quantitative I-R images with sufficient absolute accuracy, however, in addition to the high technical commitment, a high numerical application is necessary. That expenditure in time and material, and the greater dependency of the atmospherical conditions, heavily limit the routine-wise use of I-R remote-sensing procedures.

Acknowledgements:

We owe thanks to all those who contributed to the success of the programme, especially to the DFVLR and their aircraft crew, the captains and crews of the research vessels and the light vessels. We also thank the Pilot Association Weser/Jade and the Biologische Anstalt Helgoland for their friendly support. The Seewetteramt Hamburg very kindly carried out the meteorological observations and processed them for us.

Dipl.-Ozeanogr. Krause (DHI) and Dr. Krauth (DFVLR) supported us in the processing of the data on DIBIAS. Herr Kempe and Herr Höntzsch prepared the figures and took care of the editorial work. The translation into English was undertaken by Mrs. Petersitzke.

LITERATURE

Davis, Paul A. and William Viezee: A Model for Computing Infrared Transmission through Atmospheric Water Vapor and Carbon Dioxide.
J. Geophys. Res., Vol. 69, No. 8, pp. 3785 - 3794

Selby, J.E.A. and R.M. McClatchey (1972): Atmospheric transmittance from 0.25 to 28.5 µm: Computer Code Lowtran 2.
Environm. Res. Papers, No. 427, AFCLR-72-0745

Hasse, Lutz (1963): On the cooling of the sea surface by evaporation and heat exchange.
Tellus XV (1963), 4

Literature (continued)

Hasse, Lutz (1971): The Sea Surface Temperature Deviation and the Heat Flow at the Sea-Air Interface.
Bound. Layer Met. 1(1971), pp. 368 - 371

Huber, K (1978): Numerical treatment of I-R Scanner images.
(in preparation)

Nagel, H.A. (1971): A Prediction Model for the Variation of the Thermal Structure in the Ocean Surface Layer.
Texas A & M University, Techn. Rep. Ref. 71-23-T

Haney, R.L.(1971): Surface thermal boundary condition for ocean circulation models.
J. Phys. Oceanogr., Vol. 1, (1971)

Stevenson, Merrit R. and F.R. Miller (1974): Application of Satellite Data to Study Oceanic Fronts in the Eastern Pacific.
Final Report, Inter-American Trop. Tuna Comm.

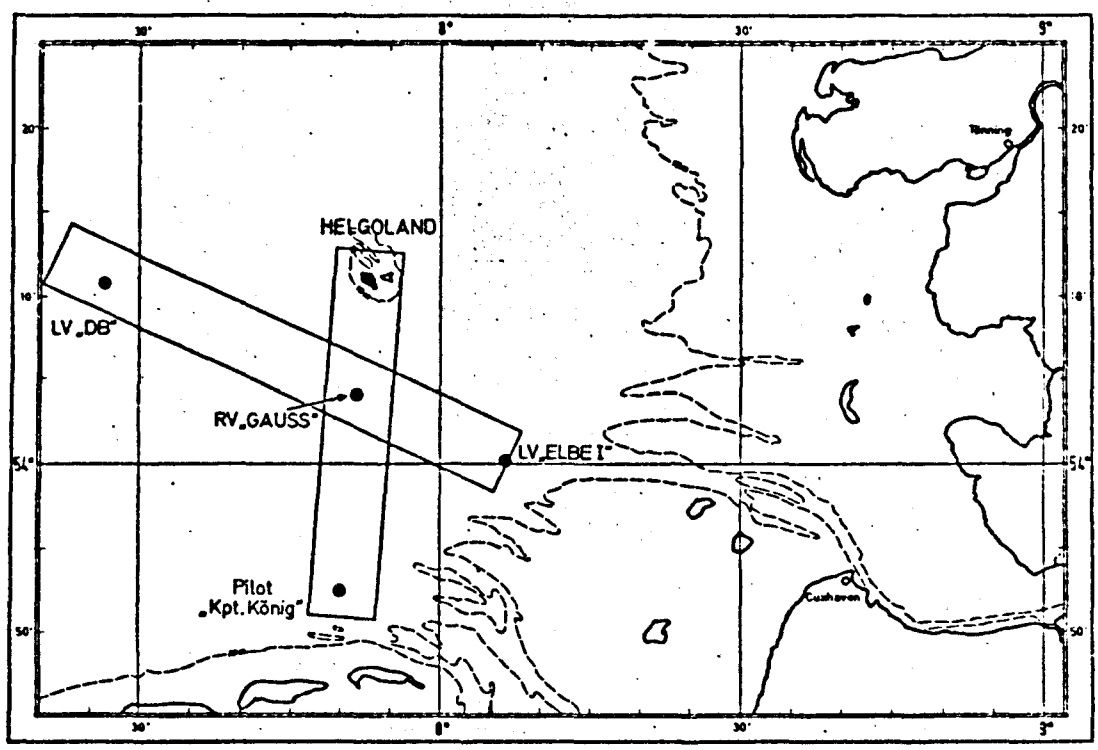

Fig. 1 Test area and flight paths

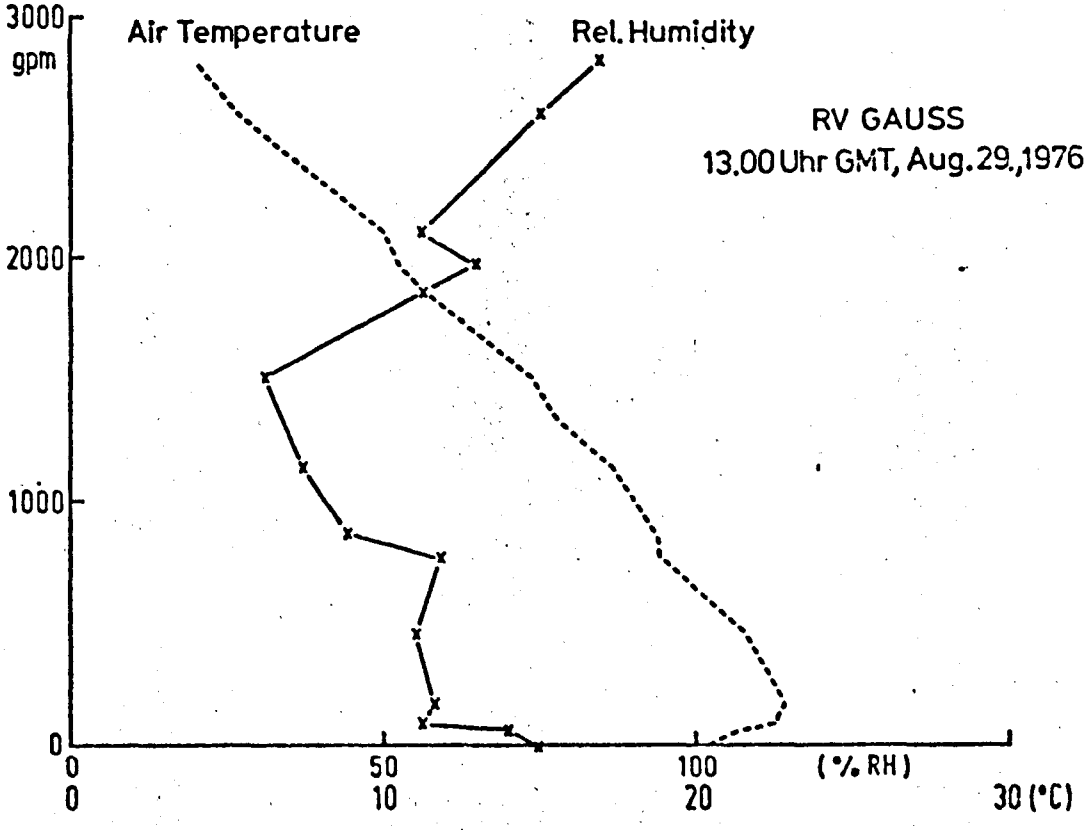

Fig. 2 Radiosonde profile, relative humidity, and temperature

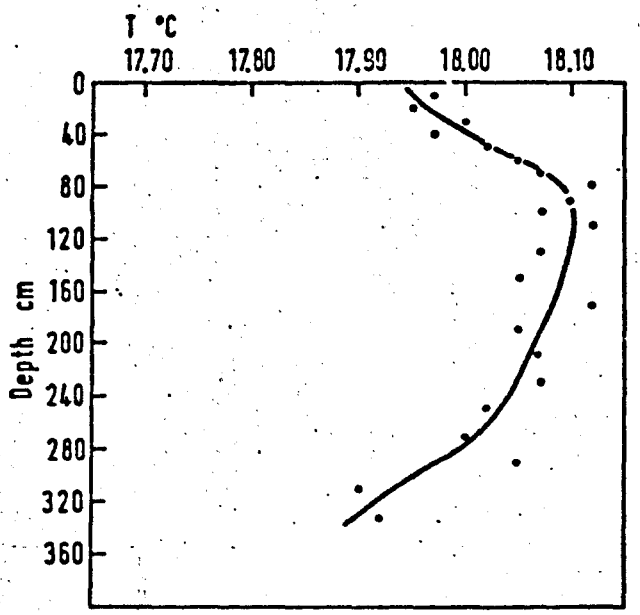

Water Temperature Profil
30.8.1976, 15.12 Uhr GMT
(Surface Rider Thermistor Chain)

Fig. 3 Near-surface water temperature profile

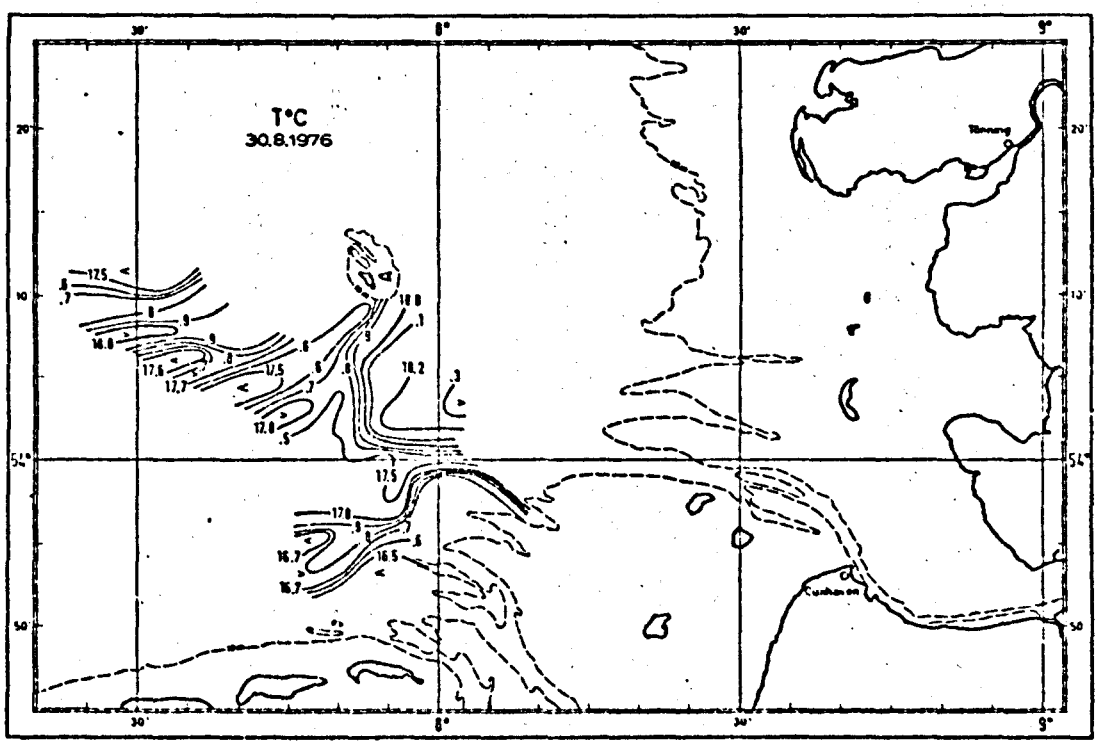

Fig. 4 Sea surface temperature distribution in the test area

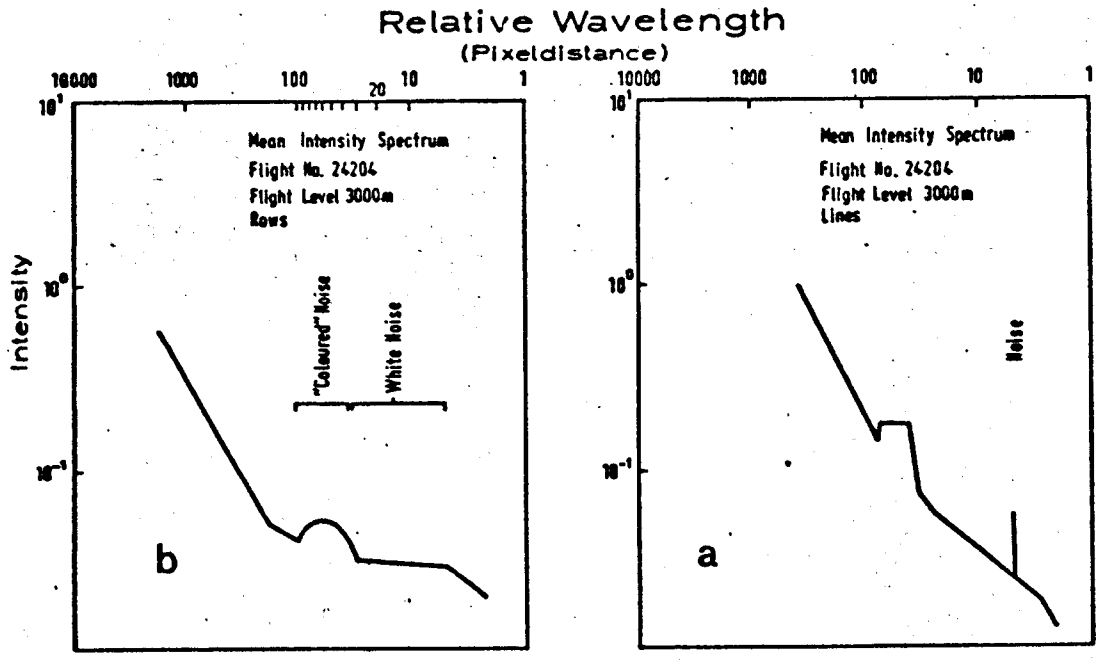

Fig. 5a Mean intensity spectrum: lines

Fig. 5b Mean intensity spectrum: rows

Filterspectren

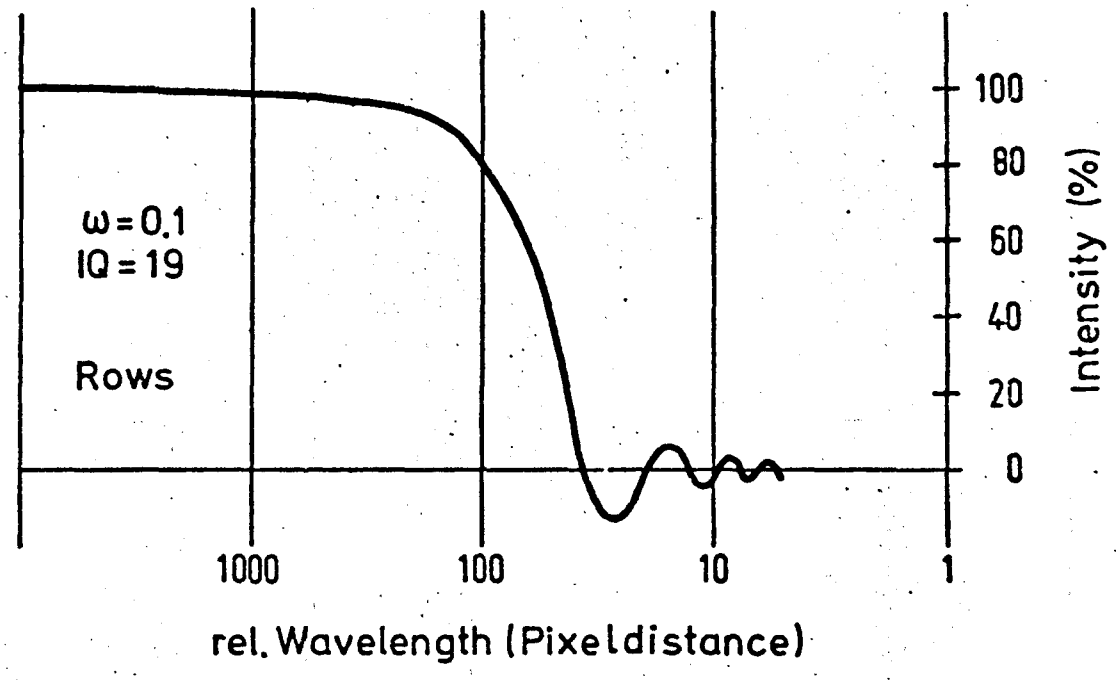

Fig. 6b Filter spectrum: rows

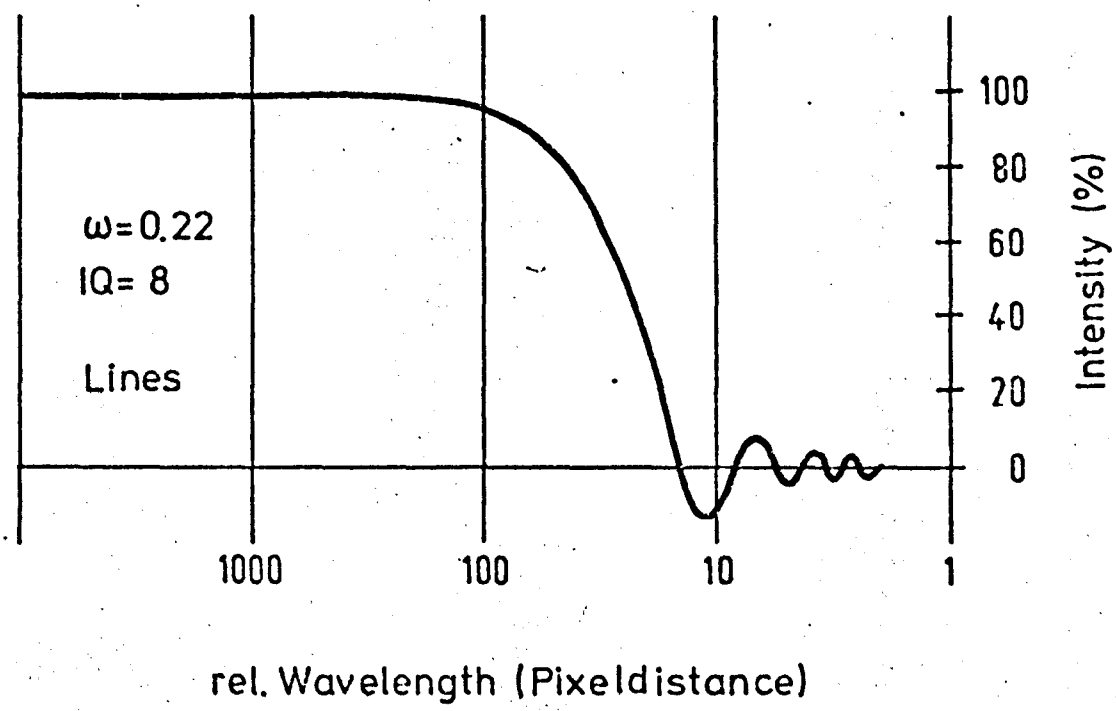

Fig. 6a Filter spectrum: lines

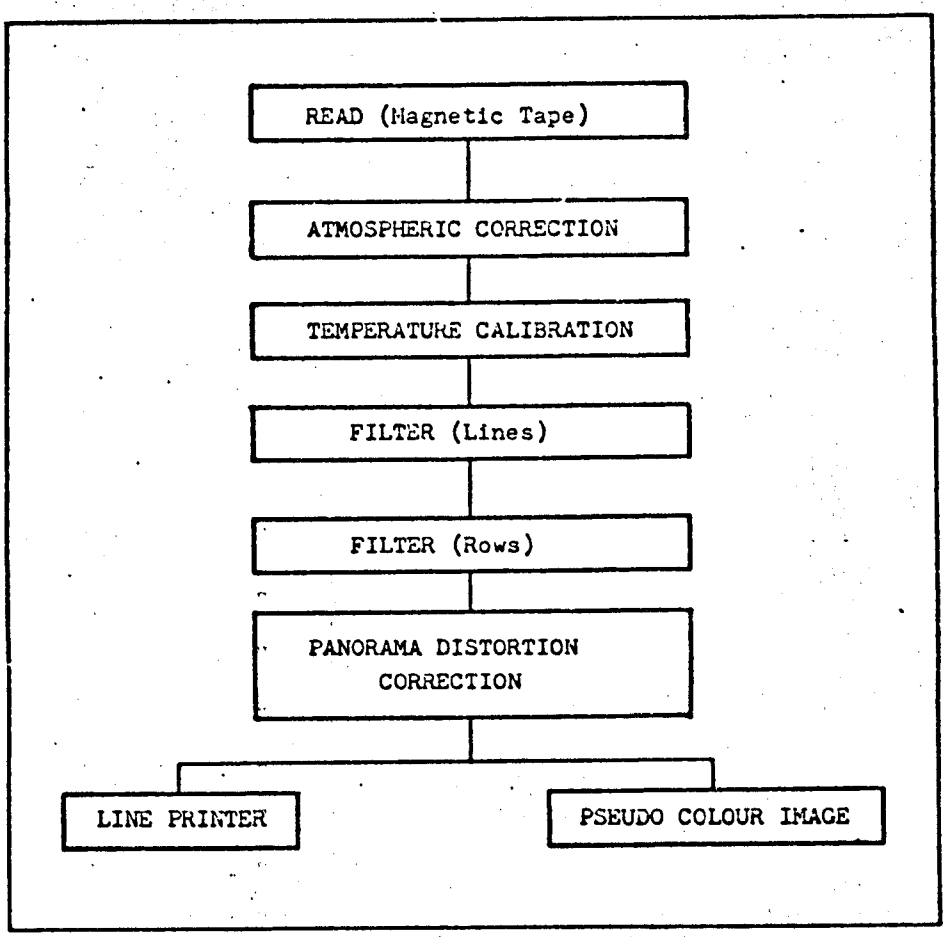

Fig. 7 Flow diagram

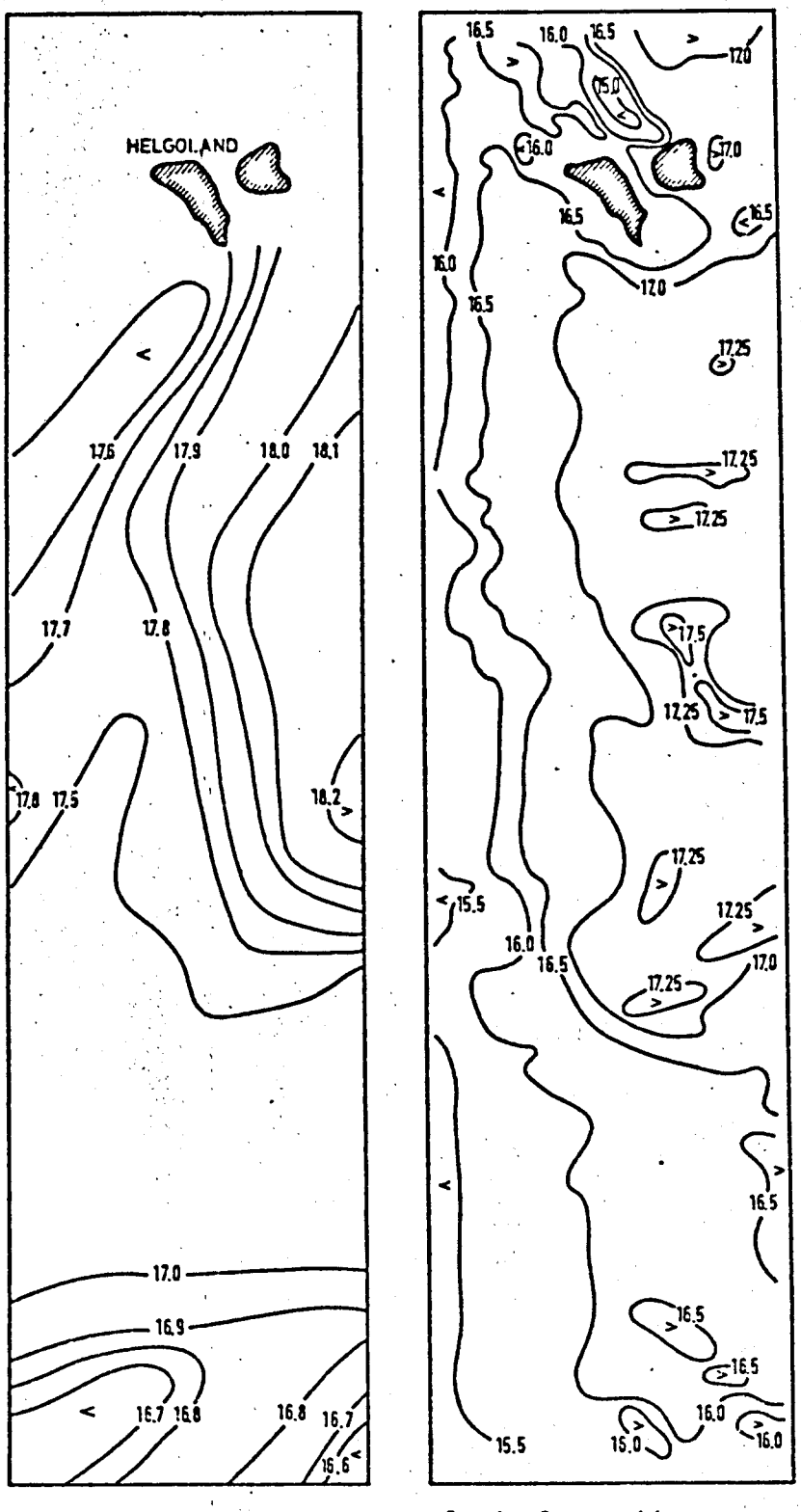

Sea Surface Temperature
30.8.1976; 07.00-11.00 Uhr, 15.15-23.00 Uhr GMT
(Thermosalinograph, Bucket)

Skin Temperature
29.8.1976; 15.06-15.12 Uhr GMT
(M^2S, Channel 11)

Fig. 8 Comparison of conventional and radiometrical temperatures